Estimated Thickness of a Fragmental Surface Layer of Oceanus Procellarum

VERNE R. OBERBECK AND WILLIAM L. QUAIDE

Space Sciences Division, Ames Research Center
Moffett Field, California 94035

Laboratory impact cratering studies have been used to analyze the relationship between the crater size and crater morphology observed on the Lunar Orbiter 1 photographs. The results indicate that the fragmental surface layer is of variable thickness in the area of the Surveyor 1 landing site on Oceanus Procellarum. It is estimated that in 85% of the area the fragmental cover is between 5 and 15 meters thick. The estimated modal thickness is in the 5- to 6-meter range, and the average thickness is from 8 to 9 meters. Differences are indicated in the average thickness between this region and other mare regions and between the maria and the highlands photographed by Orbiter 1. Such differences could have an age significance, implying that new rock surfaces on the moon have been formed at different times.

INTRODUCTION

Knowledge of the physical properties of the lunar surface has increased rapidly during the last few years. Early information about the physical characteristics of the lunar surface materials came primarily from indirect measurement techniques. Light polarization and reflection, infrared and radio-frequency thermal, and radio-frequency reflection characteristics of the lunar surface, taken together, were compatible with a model of the surface that consisted of a low-density, fine-grained deposit of varying but undertermined thickness. The three Ranger missions provided direct photographic evidence of the fine structure of the lunar surface, but the physical characteristics of the material could not be determined directly. Considerations of the geometry of the many small craters visible on the highest-resolution photographs together with experimental studies of impact cratering led to the generally held interpretation that the lunar surface was composed of loose or very low-cohesive strength materials of unknown thickness. Luna 9 and Surveyor 1 photographic missions provided more direct evidence of the existence of a low-strength lunar surface layer of fragmental nature, but they gave no information that permitted the precise measurements of the thickness of such a layer. Lunar Orbiter 1 photographs have now provided information from which the thickness of the layer can be estimated.

Gault et al. [1966*a*] observed from laboratory cratering studies inspired by the Ranger photographs that impacts against targets of fragmental materials overlying a rock substrate could produce craters with a peculiar concentric or terraced structure. They found that craters with normal spherical segment or conical geometry developed when the fragmental materials were of such thickness that the rock substrate did not interfere with crater growth.

Examination of Orbiter 1 photographs revealed that numerous craters with concentric geometry are present on the lunar surface, and that they might be used to estimate the thickness of the fragmental surface layer. Careful study of selected photographs revealed further that all fresh craters with diameters less than a few hundred meters can be structurally classified and that the crater structure is size dependent. This discovery prompted an investigation of the conditions of formation of all crater structures arising through impact against a target that consisted of fragmental material resting on a cohesive substrate. These studies show that all the morphologic classes recognized can be produced by impact if the thickness of a fragmental surface layer resting on a cohesive substrate is varied. The conditions of formation of all observed crater types are defined in this paper, and the experimental results are applied to size-frequency distribution data of each crater type observed to compute the per

cent of area-thickness distribution of the fragmental surface layer on 2980 km² of Oceanus Procellarum.

Observations

Small fresh craters observed on Lunar Orbiter 1 photographs can be classified into three morphologic types: normal, flat-bottomed, and concentric.

Figure 1 demonstrates that each morphologic type has a characteristic shadow pattern. Craters with normal geometry have either conical or spherical segment shapes as deduced from their completely arcuate shadow patterns. The flat-bottomed craters have a pronounced flat floor as indicated by single annular shadow patterns, although some contain a well-defined central mound. Concentric craters, characterized by double annular or annular arcuate shadow patterns, have a crater-within-crater structure. When the central crater is small in comparison to the outer crater, perfect concentricity results; when the central crater is larger, the outer crater appears to be terraced. Even when concentric craters are not well defined, as if they had been eroded, remnants of the inner terrace are frequently visible. Some concentric craters have polygonal rims, and a few craters larger than 400 meters display a multiplicity of inner terrace levels.

The Lunar Orbiter A −9.2b site in Oceanus Procellarum, north of Flamsteed, is densely populated with all these crater types. It was selected for detailed study because of the abundance of the three morphologic types and because of the photographic coverage of the fine surface structure of a portion of this area by the Surveyor 1 spacecraft. The area studied includes 2980 km² on nonoverlapping portions of photographs M-207 and M-201.

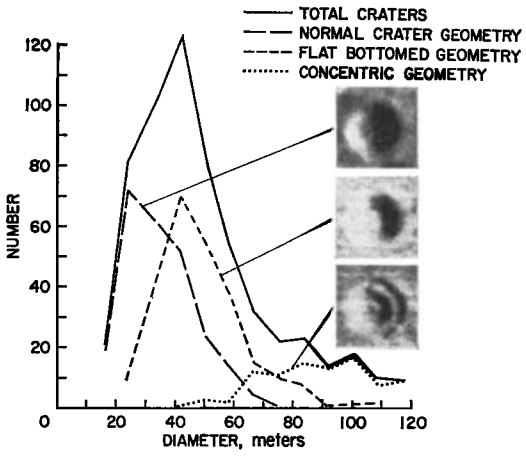

Fig. 1. Crater counts for fresh normal, flat-bottomed, concentric, and total craters of diameter D in Orbiter A 9.2b site. Enlargements of Orbiter photographs of each type are included.

Craters with diameters between 40 and 250 meters in the Lunar Orbiter A 9.2b site have been counted and classified morphologically. Only fresh craters were counted and classified, because it was thought that the structural types have a genetic significance. Craters with diameters greater than 70 meters were considered fresh if rays or halos were present. Craters smaller than 70 meters were considered fresh if crater features were sharp; rays or halos of craters smaller than 70 meters are difficult to detect under the conditions of Orbiter 1 photography.

The observed number of normal, flat-bottomed, and concentric craters of diameter D and the total observed number of craters of all classes are recorded in Figure 1 in a frequency polygon. The abrupt decrease in the total number of craters with diameters less than 40 meters is due to a lack of resolution adequate to classify craters of this size.

The absolute crater count data of Figure 1 have been recast in Figure 2 to reveal the percentage of each structural type that occurs at each crater diameter. It can be seen that most of the fresh craters with diameters less than 40 meters are apparently normal craters. Fresh craters with diameters between 40 and 70 meters are predominantly flat-bottomed, and fresh craters with diameters between 70 and 120 meters are predominantly concentric. All fresh craters with diameters between 120 and 250 meters are concentric.

Experimental Results

The observed correlation between crater size and crater shape can be readily explained as a result of meteorite impact against a surface consisting of fragmental material of variable thickness overlying a cohesive substrate.

Figure 3 shows a series of cross sections of craters produced by impact of Lexan projectiles against layered targets of fragmental surface

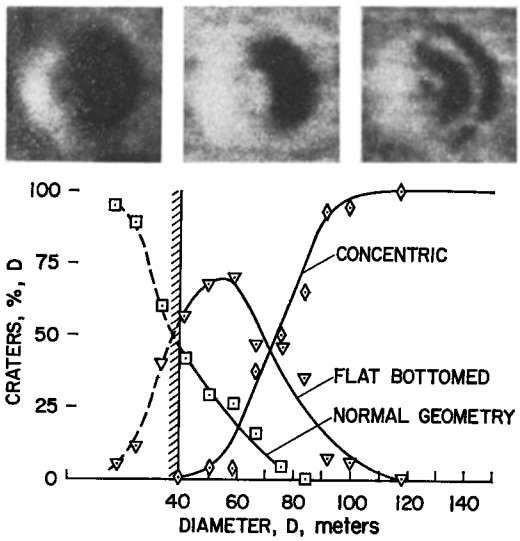

Fig. 2. Percentages of normal, flat-bottomed, and concentric craters of diameter D. Practical limits of resolution and enlargements of Orbiter photographs of each type are included.

material and cohesive substrate. All craters were produced with 0.28 ± 0.02-gram Lexan projectiles launched normal to the target surface at 1.7 ± 0.1 km/sec in a chamber evacuated to 0.5 mm Hg. The surface layers consisted of loose quartz sand of variable thickness, and the cohesive substrate of all targets was made of quartz sand cemented with epoxy resin. All cross section dimensions have been normalized to crater-rim diameter, and the boundary between the surface sand layer and the cohesive substrate is indicated on each crater section.

Figure 3 includes only selected crater sections. The complete experimental sequence has been used to define the conditions of formation of all morphologic types. The crater structure can be related to the value of a parameter R, defined as the ratio of the crater-rim diameter to the thickness of the sand layer. When R is less than about 4.25, complete crater growth occurs in the surface layer because 4.25 is about equal to the diameter-to-depth ratio of craters formed in homogeneous sand targets. When R is between 4.25 and 9.25, the cohesive substrate interferes with normal crater growth and flat-bottomed craters form. When R is about 6.3, however, the flat-bottomed crater contains a central mound. Concentric craters form when R is greater than approximately 9.25.

Each type of impact crater was photographed with an angle of illumination of 27°, similar to the lighting conditions of Orbiter 1 photographs of the A 9.2b site. The shadow pattern of laboratory impact craters shows an exact similarity to the patterns observed on the Orbiter 1 photographs. The boundaries between the morphologic classes shown in Figure 3 as $R = 6.5$ and $R = 11$ are apparent boundaries rather than the experimentally determined values of $R = 4.25$ and $R = 9.25$. This choice has been made to emphasize the fact that craters formed when R is between 6.5 and 11 appear as flat-bottomed craters under the lighting conditions of Lunar Orbiter 1. The values $R = 6.5$ and $R = 11$ are the working boundary conditions used later to determine the depth of the fragmental surface layer on the lunar surface.

Data from the same experimental sequence shown in Figure 3 also show that the crater geometry changes in a continuous manner within the flat-bottomed and concentric regimes. The ratio of the flat floor diameter to the crater-rim diameter is a function of R. Figure 4 shows that the detailed morphologic change within the flat-bottomed and concentric regimes is independent of impact angle between 30° and 90° and impact velocity between 2 and 7 km/sec. Some experiments were also done using different cohesive substrate materials. Therefore, the available experimental data suggest that the value of the parameter R is the only criterion necessary to define the conditions of formation of any morphologic type.

Impact craters were also formed in targets having interlayer density differences of as much as 300%. Flat-bottomed or concentric craters were never formed. For this reason, it is suspected that the formation of flat-bottomed and concentric craters depends only on the difference in strength between the fragmental surface layer and the cohesive substrate. In the cratering process, part of the projectile kinetic energy expended for excavation of material of a fragmental target is used to break intergranular bonds in a cohesive target. Thus, when crater growth reaches the substrate of a layered target, cratering energy may be insufficient to disrupt the bonding, and further crater growth is precluded. A flat-bottomed crater results.

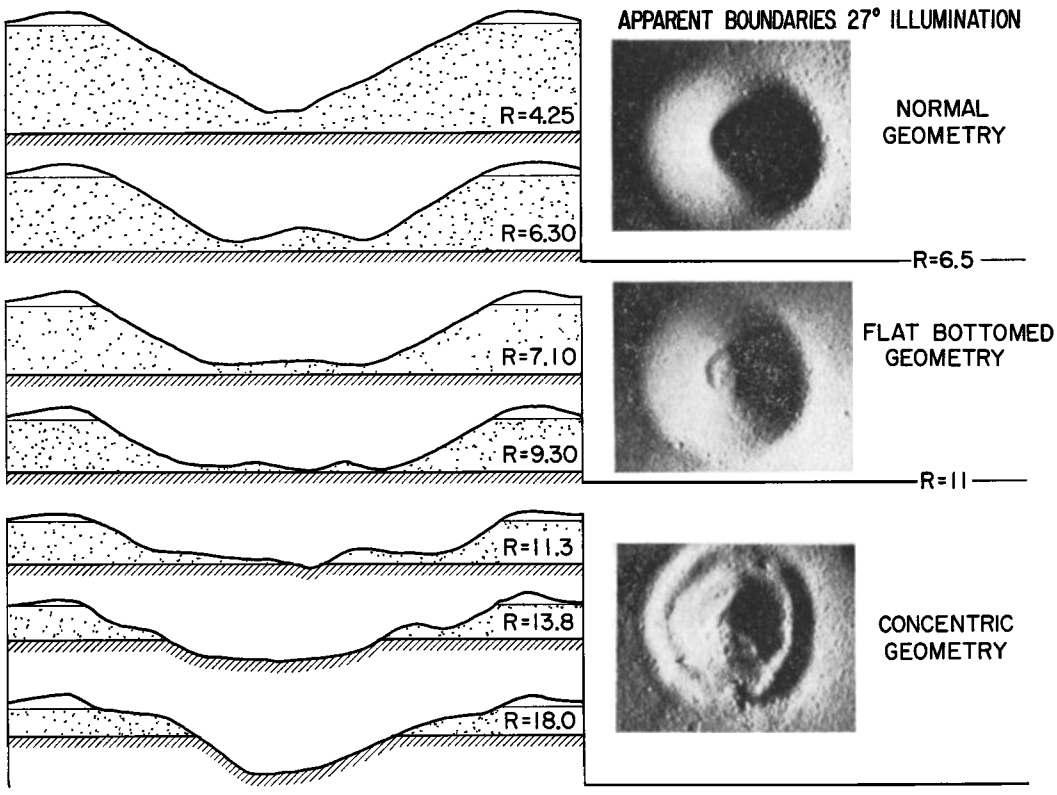

Fig. 3. Sections of laboratory impact craters (normalized to constant D) in sand targets with successively thinner, unbonded surficial layers. Relative layer thickness are expressed in terms of R = crater diameter/layer thickness. Shown also are photographs of selected craters representing the morphologic types counted and apparent boundary ratios R, separating morphologic regimes for a sun angle of 27°.

If there is sufficient energy to break the intergranular bonds of the substrate, some material can be excavated, but the growth will be less in the substrate than in the corresponding stage of crater growth in a completely fragmental material. A concentric crater results.

Discussion

Gault et al. [1966*b*] have demonstrated that the lunar surface in the area of the Luna 9 spacecraft consists of fragmental material with a thickness of at least 20 cm. *Rennilson et al.* [1966] have shown the existence of a similar fragmental surface material in the immediate vicinity of the Surveyor 1 spacecraft and have suggested that its thickness is about 1 meter. Recent results from the Luna 13 mission have indicated the presence on Oceanus Procellarum of a low-strength, low-density material of at least 20- to 30-cm depth [*Tass*, 1966]. The results reported here are consistent with these earlier results, but they also provide information on the nature of the substrate. The substrate material appears to be cohesive rock rather than permafrost. The presence of occasional multiple concentric craters with as many as three internal terrace levels would be consistent with an interpretation that the cohesive units are permafrost only if ice and ice free materials are interlayered in the uppermost part of the lunar surface. Furthermore, exposure and sublimation of ice would not leave the sharp terrace edges observed on the concentric craters. The experimental results also offer a means of estimating the distribution of fragmental surface thicknesses over a selected area on the lunar surface.

The thickness of the fragmental layer over-

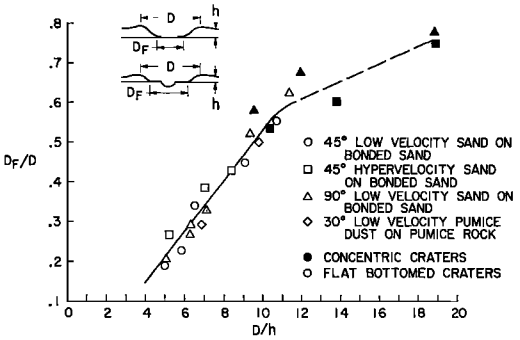

Fig. 4. The ratio, flat-floor diameter/crater diameter plotted against the ratio R for flat-bottomed and concentric craters for various conditions of impact angle, velocity, and target composition.

lying the rock unit can be estimated by means of the experimental conditions of formation of a given morphology (shown in Figure 3) and the data in Figure 2. According to Figure 3 and earlier discussion, it is seen that flat-bottomed craters observed in the A 9.2b site could have been formed under a variety of cratering conditions. The presence of a flat-bottomed crater indicates that the value of R for that cratering event is between 6.5 and 11. In a similar manner a concentric crater indicates that R is greater than 11 for that event; a normal crater indicates that R is less than 6.5. With knowledge of crater diameter and structure computed limits can be placed on the depth of the fragmental layer at the crater site.

If it is assumed that craters of a given morphology and diameter D are randomly distributed on the lunar surface, the crater counts of Figures 1 and 2 provide a normal sample of all craters of that morphology and that diameter that have been produced in the area studied. The fragmental layer thicknesses calculated from this sample of craters of diameter D are therefore a normal sample of the thickness of the fragmental layer.

For example, Figure 2 shows that 30% of all 50-meter craters on Orbiter 1 photographs have normal geometry. This means that in about 30% of the area examined the thickness of the fragmental layer must be greater than 50/6.5 or 7.7 meters. Because 5% of the 50-meter craters have concentric geometry, about 5% of the area has a fragmental layer less than 50/11 or 4.5 meters. Similarly, 65% of the 50-meter craters are flat-bottomed. Therefore, about 65% of the lunar surface area examined has a fragmental layer thickness between the limits of 50/11 and 50/6.5, or 4.5 and 7.7 meters, respectively.

Table 1 lists the results of these calculations performed for each crater diameter. The crater diameters used and listed in Table 1 are midpoints of the diameter intervals used in counting. Shown also are the 90% confidence intervals of the true percentage of lunar surface area having the indicated limits of fragmental thickness h. The 90% confidence intervals of the percentage of lunar surface area with fragmental layer thicknesses greater than h computed from the normal and concentric crater data are plotted in Figure 5. The curve has been drawn through these limits with the additional constraints imposed by the 90% confidence intervals obtained from the flat-bottomed crater data in Table 1. All data listed in Table 1 are consistent with the curve shown in Fig-

TABLE 1. Calculated Per Cent Area Thickness Distribution of Fragmental Surface Layer on Oceanus Procellarum

		Normal Geometry				Concentric Geometry				Flat-Bottomed Geometry			
Crater Diameter D, meters	N Total	N	% Area	90% Confidence Interval % Area	$h > D/6.5$	N	% Area	90% Confidence Interval % Area	$h < D/11$	N	% Area	90% Confidence Interval % Area	$h > D/11$ $h < D/6.5$
42	123	52	42.2	35–50	6.5	1	1	0–4	3.8	72	58	51–66	3.8 – 6.45
50	84	24	29	21–39	7.7	3	4	1–9	4.6	55	67	58–76	4.6 – 7.7
59	53	14	26	17–38	9.1	2	4	1–12	5 35	37	70	58–81	5.35– 9.1
67	32	5	15.6	6–28	10.3	12	38	23–54	6.1	15	47	31–62	6.1 –10.3
76	22	1	4 5	0.3–20	11.7	11	50	31–69	6.9	10	45	27–66	6.9 –11.7
84	23	0	0	0–13.5	12.9	15	65	48–82	7 6	8	35	18–55	7.6 –12.9
92	14	0	0	0–21	14.2	13	92	69–100	8.35	1	7	0.3–3.1	8.35–14.2

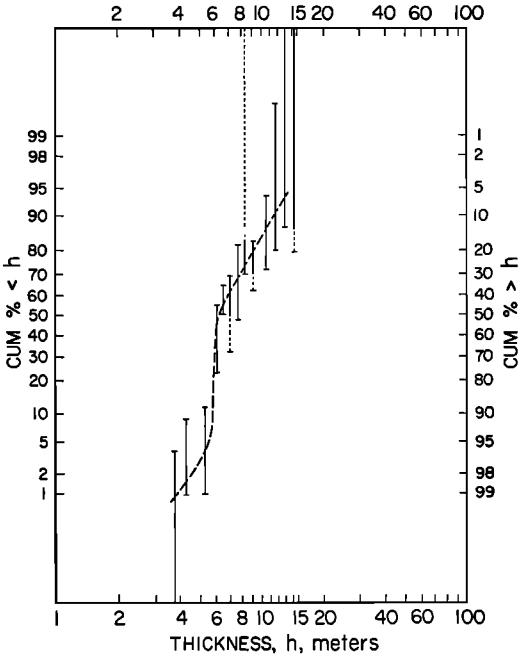

Fig. 5. Cumulative curve of the per cent area thickness distribution of the fragmental layer on the A 9.2b site. Error bars are 90% confidence intervals based on concentric and normal geometry craters, assuming a normal sample distribution.

ure 5. The data indicate with 90% confidence that the cumulative per cent area with fragmental thickness $>h$ in the Lunar Orbiter A 9.2b site in Oceanus Procellarum must be very close in the value shown by the curve in Figure 5. Thus, 85% of the area has an estimated fragmental thickness between 5 and 15 meters. The estimated modal thickness is in the 5- to 6-meter range, and the average thickness is in the 8- to 9-meter range. The distribution is peaked in the 5- to 6-meter range and skewed toward greater thickness.

Subjective errors in crater classification and counting appear to be minimal. Each of the authors counted separate but equal areas of the Lunar Orbiter A 9.2b site and obtained identical size-frequency distributions for each geometric type. The photographs were exchanged and the process was repeated with the same results. It is useful to consider the effect of the maximum possible error in selection of the working boundary values of R. Even if the experimental boundary values are used in the computations of Table 1, the computed per cent area of fragmental thickness distribution is not significantly altered. Calculations show that the form of the curve shown in Figure 5 would not change under these conditions but that the curve would be shifted to greater thickness. For example, 85% of the area would have an estimated fragmental thickness between 6.5 and 20 meters, and the modal thickness would be in the 6.5- to 7.5-meter range.

Detailed studies of the size distribution of craters of the three morphologic types have been confined to an area in Oceanus Procellarum. All medium-resolution Orbiter 1 photographs have been scanned, however, to observe the distribution of concentric craters, a crater type which can be easily detected under all the lighting conditions of Orbiter 1 photography. Concentric craters are present on all mare surfaces, but the number-size distribution is different for different areas. In the areas where the density of concentric craters is lower than the density observed on Oceanus Procellarum, the minimum and average size observed are larger. This indicates that the fragmental layer is thicker in these areas. Where the fragmental layer is thicker, only the larger craters have concentric structure. Concentric craters are less numerous because there are fewer large cratering events. The observed variations in size-frequency distributions of concentric craters from one mare to another are compatible with significant variation in the average thickness of the fragmental layer from one mare to another.

To interpret the variation of average thickness of the fragmental layer within the maria it is necessary to consider the origin of the fragmental material. It has long been recognized that impact cratering and impact comminution have been important processes on the lunar surface. *Gault et al.* [1963] showed that the principal result of the impact process is the production of fragmental material. If we assume that a constant flux of impacting bodies is the important mechanism for producing a fragmental layer, the average thickness of the layer in any area is related to the elapsed time since formation of a new rock surface. Variations of the average thickness of the surface layer in widely separated areas on the moon can be explained by the formation of new rock surfaces at different times in those areas.

On the other hand, sporadic contributions of large amounts of volcanic debris must also be considered as a source of fragmental debris. *O'Keefe and Cameron* [1962] and *Lowman* [1963], for example, have suggested that ash flows or tuff deposits have covered significant portions of the maria. If there have been significant sporadic contributions of volcanic debris, the thickness of the fragmental layer would not have precise time significance.

Scans of the highlands have shown that there is a lack of concentric craters in these areas. The absence of this kind of crater could indicate that a surficial fragmental layer of detectable thickness has not been formed. A more reasonable interpretation is that a fragmental layer exists and is so thick that craters large enough to reflect this thickness are extremely rare, or that on this scale the strength of the surficial and subsurface materials is effectively the same. If the highland surfaces have a fragmental layer so thin that it cannot be detected, the near-surface hard rock material is younger than the substrate material of the maria. This situation does not appear feasible in view of all previous evidence on the relative ages of the highlands and the maria [*Baldwin*, 1963]. It is therefore assumed that the lack of concentric craters on the highlands means that a fragmental layer exists there and is thicker than the fragmental layer on the maria. This implies that the highland substrate is older than the substrate material of the maria.

Variations in thickness of the surface layer from one mare to another indicate that rock-forming events have taken place on the maria at different times. For this reason, it is probable that intermittent rock-forming events have occurred at one place, resulting in alternating units of rock and fragmental material. This interpretation is supported by the presence of a few 500-meter-diameter concentric craters on the mare surfaces photographed by Lunar Orbiter 1. As many as three inner terrace levels have been observed. Such multiple concentric craters suggest that three alternating units of fragmental material and hard rock could occur in the uppermost 100 meters of the mare at the crater site.

Summary

Experimental laboratory results have been used to interpret the sequence of crater structures seen on Oceanus Procellarum and to determine the detailed distribution of thickness of surficial fragmental materials. The analysis indicates that 85% of the area considered has a surficial thickness between 5 and 15 meters. The estimated modal thickness is in the 5- to 6-meter range; the average thickness, in the 8- to 9-meter range. The interpretation of the surficial layer as a fragmental material is based on earlier evidence obtained from the analysis of photographs of the Luna 9 and Surveyor 1 sites and evidence from the Luna 13 mission.

It has also been shown that the estimated average thickness of the fragmental layer varies from one mare to another and that it is likely that the highlands contain an even thicker layer of fragmental material than the maria.

If the fragmental layer is assumed to be of impact origin, the thickness of the fragmental stratigraphic unit is related to the age of the unit. The differences in thickness from place to place on the maria and from maria to highland might, therefore, indicate differences of elapsed time since the last production of new rock surfaces in those areas.

Furthermore, it is reasonable to expect that the production of new rock surfaces has been repeated from time to time in the same place, leading to a complex stratigraphic sequence of alternating units of hard and fragmental rocks. The discovery of multiple concentric craters on Oceanus Procellarum indicates that such a sequence is to be expected.

References

Baldwin, Ralph B., *The Measure of the Moon*, University of Chicago Press, Chicago, Illinois, 1963.

Gault, D. E., W. L. Quaide, and V. R. Oberbeck, Interpreting Ranger photographs from impact cratering studies, chapter 6, in *The Nature of the Lunar Surface*, edited by W. N. Hess et al., The Johns Hopkins Press, Baltimore, Maryland, 1966*a*.

Gault, D. E., W. L. Quaide, V. R. Oberbeck, and H. J. Moore, Luna 9 photographs: evidence for a fragmental surface layer, *Science, 153*, 985–988, 1966*b*.

Gault, D. E., E. M. Shoemaker, and H. J. Moore, Spray ejected from the lunar surface by meteoroid impact, *NASA Publ. D-1767*, Washington, D. C., 1963.

Lowmann, P. D., Jr., The relation of tektites to lunar igneous activity, *Icarus, 2*, 35–48, 1963.

O'Keefe, J. A., and W. S. Cameron, Evidence from the moon's surface features for the production of lunar granites, *Icarus, 1,* 271–285, 1962.

Rennilson, J. J., J. L. Dragg, E. C. Morris, E. M. Shoemaker, and A. Turkevich, Lunar surface topography, chapter 3, in Surveyor 1 Mission Report, part 2, Scientific Data and Results, *Jet Propulsion Lab. Tech. Rept. 32–1023,* 1966.

Tass Press Releases, Dec. 25–31, 1966, *NASA, Goddard Space Flight Center Transl. ST-PR-LPS-10 545,* Jan. 4, 1967.

(Received March 24, 1967.)